NATIONAL ADVISORY COMMITTEE FOR AERONAUTICS

TECHNICAL NOTE 2484

EFFECTS OF COMPRESSIBILITY ON THE FLOW PAST A TWO-DIMENSIONAL BUMP

By W. F. Lindsey and Bernard N. Daley

Langley Aeronautical Laboratory
Langley Field, Va.

Washington
April 1952

1P

NATIONAL ADVISORY COMMITTEE FOR AERONAUTICS

TECHNICAL NOTE 2484

EFFECTS OF COMPRESSIBILITY ON THE FLOW PAST A TWO-DIMENSIONAL BUMP[1]

By W. F. Lindsey and Bernard N. Daley

SUMMARY

An investigation has been conducted to determine experimentally the effects of compressibility on the flow past a bump and to compare the experimentally determined results with theory. Pressure measurements and schlieren photographs were made over a large Mach number range of the flow past two bumps having thickness-chord ratios of 0.10 and 0.30.

The results of the investigation indicated that the effects of compressibility on the flow past these specially shaped profiles or bumps were in agreement with results of previous investigations on airfoils. Reasonably good agreement was found between the experimental results and the symmetrical type of theoretical solution of the flow past bumps except over the rear half of the models at supercritical Mach numbers. This disagreement between experiment and theory suggested that an asymmetrical type of theoretical solution would be necessary to obtain agreement with the real flow. Such a solution would probably introduce mathematical discontinuities in the flow. The results of the investigation also showed that the "limiting" Mach number had no practical significance in relation to the formation of compression shocks. The theory does yield information with regard to the extent of the supersonic-flow field over the forward part of the model at Mach numbers up to the limiting value.

INTRODUCTION

A theoretical study of the flow of a compressible fluid past two-dimensional symmetrical bumps of various thicknesses is given in reference 1. In reference 1 an iteration process credited to Ackeret (reference 2) is used; this process extends the Prandtl-Glauert relation (references 3 and 4) to higher-order terms. Reference 1 shows that the addition of the second- and third-order terms produced an increase in the predicted effect of compressibility on the maximum negative pressure coefficients; the resulting effect was in good agreement with that obtained

[1]Supersedes recently declassified RM L6K12b "Effects of Compressibility on the Flow Past a Two-Dimensional Bump," by W. F. Lindsey and Bernard N. Daley, 1947.

from Von Kármán-Tsien relation (reference 5). Reference 1 also gives a theoretical indication of a "limiting" Mach number beyond which potential flow or flow without shock did not exist. The amount by which the limiting Mach number exceeded the critical Mach number increased as the thickness-chord ratio increased.

The profile of the shape for which the theoretical study of the flow was made (reference 1) was such that reasonable agreement could be expected between the real flow at low speeds and the potential flow. An investigation was made, therefore, in the Langley rectangular high-speed tunnel to determine experimentally the effects of compressibility on the flow of a real fluid past this type of bump and to compare the experimentally determined results with the results obtained by perfect-fluid theory.

Models of 10- and 30-percent thickness were investigated. The thinner model corresponded to approximately the middle of the thickness range included in the theoretical study, whereas the thicker model was somewhat beyond the limits of that range. The investigation of the thick model presented an opportunity to compare two complementary theoretical methods for calculation of subsonic flows: namely, the Poggi method and the Ackeret iteration process. For thick bodies, for which the critical Mach number is small, the Poggi method should yield the more accurate result because the shape factor has a greater effect than the compressibility of the fluid. For thin bodies, for which the critical Mach number is high, the Ackeret process should yield the more accurate solution because the effect of compressibility of the fluid is greater than the shape effect. (See reference 1.)

The experimental investigation consisted of pressure measurements and schlieren photographs of the flow past the two 4-inch-chord models. The pressure measurements were made at Mach numbers from 0.22 to the choking Mach number of the tunnel. The schlieren photographs were obtained in the supercritical-speed region. Inasmuch as the theoretical study was restricted to an angle of attack of 0° to avoid the occurrence of a stagnation region at the sharp leading edge of the symmetrical shape, the present investigation was conducted so that this condition would be satisfied.

SYMBOLS

M	stream Mach number
M_{cr}	critical Mach number (stream Mach number at which sonic velocity is attained locally, as at model surface)

q	stream dynamic pressure $\left(\frac{1}{2}\rho V^2\right)$
p	stream static pressure
p_l	local static pressure (as at model surface)
P	pressure coefficient $\left(\frac{p_l - p}{q}\right)$
P_{max}	maximum negative pressure coefficient at model surface
P_{cr}	critical pressure coefficient $\left(\frac{0.528H - p}{q}\right)$; corresponds to $M = 1.0$ at model surface
H	stream total pressure
H_w	total pressure in wake of model
ΔH	theoretical decrease in total pressure through a normal shock
y/c	distance from surface to point in local flow field where $M = 1.0$, percent model chord
x_s	location of forward station on model at which stream velocity ($P = 0$) is attained
c_d	section drag coefficient
γ	ratio of specific heats
ρ	stream mass density
V	stream velocity
c	chord of bump
t	thickness of bump

Subscripts:

10	10-percent bump
30	30-percent bump

APPARATUS AND METHODS

The present investigation was conducted in the Langley rectangular high-speed tunnel, which is a nonreturn induction-type tunnel having a 4- by 18-inch test section (fig. 1(a)). The 4-inch dimension of this tunnel is fixed, but the two narrow walls are flexible and permit the height (18 in. at test section) to be varied in order to adjust the pressures along the tunnel axis.

Tests were made on only one surface of each model because the models were symmetrical and were tested at an angle of attack of 0°. The surfaces or bumps were attached to a long flat support plate installed along the tunnel center line and spanning the 4-inch dimension. The two bumps, representing 10-percent- and 30-percent-thick models, were attached to opposite sides of the support plate at the test-section level, the chords of the models coinciding with the surfaces of the plate. The plate thus assured the proper attitude of the model with respect to the flow. The thickness of the boundary layer on the support plate at the test-section level was expected to be small because of the favorable pressure gradient ahead of the model location, and a thin boundary layer was indicated by total-pressure measurements normal to the tunnel walls at the test section.

The installation is shown schematically in figure 1(b). This installation divided the tunnel into two relatively independent channels of flow. The Mach number of the flow in each channel was determined independently by means of calibrated static-pressure orifices located upstream of the test section. The axial static-pressure gradient at the test-section level with the models removed was not appreciable along the support frame for Mach numbers below 0.85; along the tunnel wall above the model location at a Mach number of 0.85 a variation from -1 to 3 percent of the Mach number of the flow was indicated.

The 10- and 30-percent bumps of 4-inch chord completely spanned the test section. Each model had one chordwise row of static-pressure orifices installed on the model surface at the semispan station. Model profiles, orifice locations, and model-support assembly are shown in figure 2.

Data were obtained by measurements of the chordwise static-pressure distribution along the surface of the bumps and of the total-pressure variation across the wakes of the bumps. The pressure measurements were obtained at Mach numbers from 0.22 to the choking Mach number for each bump. The choking Mach number was 0.86 for the 10-percent bump and 0.73 for the 30-percent bump. Additional information on the flow past the bumps was obtained at supercritical Mach numbers in the form of schlieren photographs.

TUNNEL-WALL EFFECTS

The existence of constriction effects in high-speed tunnels has been shown experimentally (reference 6) and the problem has been investigated theoretically (reference 7). The theoretically derived correction, based on the assumption of small induced velocities at subcritical Mach numbers (see also reference 2), should provide an indication of the magnitude of the tunnel-wall effects. The theoretically indicated errors for both bumps at their critical Mach number are as follows:

10-percent bump
$$\text{Corrected } M = M \times 1.010$$
$$\text{Corrected } q = q \times 1.013$$

30-percent bump
$$\text{Corrected } M = M \times 1.012$$
$$\text{Corrected } q = q \times 1.020$$

The theory thus indicates that the correction at the critical Mach number is small. Because the indicated correction is small and would have no significant effect on the main conclusions obtained from the present investigation, the experimental data presented herein are uncorrected for tunnel-wall effects.

The choking phenomenon is an additional factor that enters into the problem of wind-tunnel testing at high subsonic Mach numbers. At the choking Mach number sonic velocities extend from model to tunnel wall, and the static pressure is lower behind the model than ahead of the model; thus large gradients are produced in the static pressure (reference 6). The resulting flow past the model is unlike any free-air condition, and data obtained at the choking Mach number are therefore of questionable value and are not presented herein.

RESULTS

A comparison of the pressure distributions along the profile of the 30-percent bump at a Mach number of 0.50 derived by the theoretical methods of Poggi and of Ackeret is presented in figure 3.

The basic results of the experimental investigation are presented in figures 4 to 7. The variations with Mach number of the pressure distributions that were determined experimentally are presented in figure 4 for the 30-percent bump and in figure 5 for the 10-percent bump. The theoretically derived pressure distributions are included in figures 4 and 5 for comparison with the experimental results. The flow past the

two bumps at high Mach numbers is shown by the schlieren photographs presented as figure 6. Additional information on the effects of compressibility on the flow past the 10-percent bump is shown in figure 7 as the variation with Mach number of the pressure coefficient at stations located various distances above the surface of this bump at the 0.50-chord station.

The variation with Mach number in the estimated normal shock loss for the 10-percent bump is presented in figure 8, and the total pressure variation across the wake of the 10-percent bump at several Mach numbers is shown in figure 9. The effect of compressibility on the location of the station at which stream velocity ($P = 0$) was attained on the forward part of the model is shown for both bumps in figure 10.

DISCUSSION

Comparison of Experiment with Theory

Poggi's and Ackeret's methods.- Poggi's method yields the components of the fluid velocity in the form of a power series in stream Mach number. The coefficients of the various powers of stream Mach number are exact and valid for all values of thickness. The method of Ackeret, however, yields the components of the fluid velocity in the form of a power series in thickness (reference 1). At high subcritical Mach numbers, therefore, the more satisfactory solutions of the flow past thin models should be obtained by the method of Ackeret, whereas Poggi's method should yield the more satisfactory solutions for thick models such as the 30-percent bump. A comparison is given in figure 3 of the pressure distributions obtained by these two methods for the 30-percent bump at a Mach number of 0.500. From the appearance of wriggles in the pressure distribution derived by the method of Ackeret this method is deduced to be inaccurate for 30-percent bumps, as was expected. In the comparisons between theoretical and experimental results that are given herein the method of Poggi is used, therefore, for the 30-percent bump, whereas Ackeret's method is used for the 10-percent bump.

Subcritical Mach number range.- An examination of the theoretical and experimental pressure distributions at low speeds on the thick bump (fig. 4(a)) and the thin bump (fig. 5(a)) discloses two disagreements. The dissymmetry in the experimental pressure distribution over the front and rear parts of these models can be attributed to viscosity in the real fluid that produces a change in the flow as a result of the growth of the boundary layer. A difference between the theoretically and experimentally determined maximum negative pressure coefficients could be expected as a result of the effects of the boundary layer from the support plate and the simplifying assumptions (such as the assumption of a

perfect fluid) that were made in the theoretical analysis. Closer agreement between theory and experiment could have been obtained at the given speed (M = 0.225) had the theoretical pressure distributions been determined for slightly thinner models; namely, 8.3-percent and 27-percent bumps.

Inspection of the experimental pressure distributions in the subcritical Mach number range (figs. 4(a) and 4(b) and figs. 5(a) to 5(c)) indicates that the effect of compressibility on the pressures acting on these bumps is in good agreement with the theoretically predicted effect; the agreement for the thin bump is closer than for the thick bump. The theory, however, slightly underestimates the rate of increase with Mach number of the maximum negative pressure coefficient P_{max}, even for the thin model.

Supercritical Mach number range.- The pressure diagrams of figure 4 indicate that separation of the flow occurred in the supercritical speed range. This indication is substantiated by the schlieren photographs of the flow past the 30-percent bump (fig. 6). Pressure-distribution diagrams and schlieren photographs further show that as the Mach number is increased, P_{max} decreases while the shock position is not appreciably affected; these effects result from the extensive separated flow condition.

Separation of the flow from the 10-percent bump, as shown by the schlieren photographs (fig. 6) is not appreciable for Mach numbers less than approximately 0.81. At somewhat higher Mach numbers separation, of a much lesser degree than the separation from the 30-percent bump, appears to start at the base of the shock and could therefore be expected to have little or no effect on the flow ahead of the shock.

A comparison between the experimental and theoretical pressure-distribution diagrams for the 10-percent bump at supercritical Mach numbers (fig. 5) shows that the experimentally determined values of dP_{max}/dM were larger than the theoretical values (also shown in fig. 7); a large disagreement, however, occurred in the shapes of the pressure distributions. The divergence between the theoretical and experimental distributions increased as the Mach number increased above a value of 0.785 as a result of the rearward movement of both the position of P_{max} and the "discontinuity" in the experimental pressure distribution. The positions of these pressure discontinuities are in good agreement (within 0.03c) with the positions of the shocks shown in the schlieren photographs of figure 6.

If the adiabatic gas law, Bernoulli's equation for compressible flows, and the equation of continuity (conservation of mass) are combined, the following relation between flow area s and pressure p within a stream tube can be obtained:

$$\frac{ds}{s} = \frac{1 - M^2}{\gamma M^2} \frac{dp}{p}$$

where γ is the ratio of specific heats.

This relation shows that where the area of the stream tube is expanding (positive ds) compressions (positive dp) occur if the local flow is subsonic ($M < 1$), but if the local flow is supersonic ($M > 1$) expansions (negative dp) occur.

The foregoing relation, exact for flow within a stream tube, should be expected to indicate the direction of pressure change in two-dimensional flow. At subcritical speeds the shape of the pressure distribution is in agreement with this relation, as was expected. The agreement with the relation indicates that the streamlines have less curvature than the surface of the model. At supercritical Mach numbers, however, the assumption of a symmetrical solution in the theoretical study (reference 1) requires the streamlines to have more curvature than the surface in the region of supersonic flow. This theoretical requirement is not physically tenable in the flow over the rear part of the model and consequently the position of P_{max} could be expected to move rearward at supercritical speeds as shown by the experimental results. The pressure at the rear of the model, however, is high relative to the pressure in the local supersonic flow region, and this condition necessitates a compression of the fluid. All available information has shown that compressions of fluids moving at supersonic velocity are accompanied by shocks and consequently by energy losses. The compression shocks are evident in the schlieren photographs of figure 6.

The foregoing considerations indicate that the theoretical pressure distributions at supercritical Mach numbers cannot even approximate a true picture of the flow conditions over the rear of the model. The considerations further lead to the possibility that an asymmetrical type of theoretical solution would be necessary to obtain agreement with the real flow, and a mathematical solution of this type of flow could include discontinuities.

Shock losses.- The losses through shocks in two-dimensional flow are dependent on three factors: namely, the intensity of the shock, the distance the shock extends normal to the chord into the flow above the model, and the variation in intensity of the shock along this distance. The first factor obtained from measured values of P_{max} (fig. 7) and from the theoretical loss in total pressure through normal shocks (reference 8) is presented in figure 8(a) as the loss in total pressure in terms of dynamic pressure $\Delta H/q$. The factor $\Delta H/q$ is the theoretical loss incurred in a flow through a normal shock in one dimension and is only an approximate representation for the loss in two dimensions. The

second factor can be represented by the extent of the supersonic-flow region above the surface of the model y/c. The experimental values of y/c, obtained from measured static pressures in the flow field above the 0.5-chord station (fig. 7) are shown by figure 8(b) to be in good agreement with the theoretically derived values of reference 1.

The product of y/c (experimental) and $\Delta H/q$ (presented in fig. 8(c)) gives an estimated shock-loss variation for one side of the 10-percent bump. Figure 8(c), however, does not include the third factor; that is, the variation in shock intensity or loss through shock along the distance y/c. Consideration of the velocity gradient in the flow above the 10-percent bump (see fig. 7) indicates that the loss through the shock varies from a maximum value near the surface of the model (fig. 8(a)) to 0 at a distance y/c from the model where the local Mach number is 1.0. Figure 7 and the measured total pressure variation across the wake of the 10-percent bump (fig. 9) indicate that the effect of compressibility on this third factor is small for the model and the Mach number range considered. The third factor could be approximated therefore by a constant (less than 1), the effect of which would change only the numerical scale in figure 8(c).

The estimated normal-shock loss (fig. 8(c)) indicates that the critical Mach number (0.756) can be exceeded by 6.5 percent of the velocity of sound before the loss or drag increment attains a value of 0.01 as a result of shock alone. The test points in figure 8(c) are the measured increments in drag coefficient above the value obtained at a Mach number of 0.75 (obtained as from fig. 9). The delay in loss shown by these test points is in good agreement with the estimated shock loss.

Figure 8 illustrates that the assumption that shocks form at M_{cr} is in accord with the phenomena that occur and does not necessitate an abrupt increase in losses or drag at M_{cr}. The estimated shock loss, however, does not include the additional loss from flow separation that is generally encountered at supercritical speeds. (See 30-percent bump in fig. 6 and references 9 and 10.)

Stream velocity station x_s.- The existence of an effect of compressibility on the station at which stream velocity occurs x_s (fig. 10) indicates a limit to the speeds to which the low-speed pressure-distribution diagrams can be extrapolated by the theoretically derived methods in general use. The various theoretical methods of extrapolation, namely, Prandtl-Glauert (references 3 and 4), Von Kármán-Tsien (reference 5), and Temple-Yarwood (reference 11) give

$$\frac{dx_s}{dM} = 0$$

Calculations by Ackeret's and Poggi's methods (reference 1), however, show that x_s moves toward the chordwise position of P_{max} as the Mach number is increased. The movement, which by derivation is independent of viscous effects, is small at subcritical Mach numbers but increases rapidly as the critical Mach number is exceeded. By the comparison in figure 10 the effects of compressibility on x_s for the bumps as determined by experiment and by theory are shown to be in very good agreement.

The movement with increasing Mach number of x_s toward the location of P_{max} and the increase in dx_s/dM with increased thickness-chord ratio (fig. 10) is in agreement with the results of pressure-distribution measurements on airfoils (reference 12) and has been referred to as being comparable to increases in thickness.

These experimental and theoretical results indicate that the usual methods of extrapolating low-speed pressure distributions for bodies having finite induced velocities are defective for values of pressure coefficient at or near zero.

Limiting Mach number.- The theoretical pressure-distribution diagrams at supercritical Mach numbers were justified by a theoretical indication of a limiting Mach number, beyond which potential flow can no longer exist (reference 1). Flows without shock were thus assumed to occur at Mach numbers below the limiting value, even though supersonic velocities were attained locally within the flow.

The experimentally determined flow in the region of compression over the rear of the model is in complete disagreement with theory. In connection with the formation of shock, therefore, the limiting Mach number has no significance. Some agreement between theory and experiment is indicated at supercritical Mach numbers, however, on the flow over the forward part of the model (figs. 8(b) and 10(b)). The limiting Mach number therefore may be applicable to the flow in the region of expansion ahead of the low-speed location of P_{max} but is inapplicable to the region of compression and consequently to the formation of shock for which M_{cr} retains its practical significance.

Comparison of Flow past Bumps and Airfoils

General.- The effects of compressibility on the flow past the bumps at subcritical speeds, as shown by pressure distributions and schlieren photographs, are in accord with previous airfoil investigations (references 9, 10, and 12).

At supercritical speeds the effects of compressibility on the value and position of P_{max} differ for the two bumps. For the 30-percent bump

dP_{max}/dM is negative and the position of P_{max} is approximately constant throughout the supercritical speed range; for the 10-percent bump, however, dP_{max}/dM is positive and the position of P_{max} continues to move downstream with increasing Mach number. These differences may be attributed to a very large difference in the extent of the separated flow from the two bumps, the 30-percent bump naturally having the larger separated flow region.

Pressure distributions and schlieren photographs obtained from airfoil investigations are in very good agreement when compared with these experimental results on the basis of comparable adverse pressure gradients (see references 9, 10, 12, and 13).

Disturbances and pressure discontinuities.- The critical Mach number M_{cr} is important because it marks the end of the subcritical speed range, in which serious adverse effects of compressibility are not encountered.

Various methods, including inspection of schlieren photographs, have been used to determine M_{cr}. The results of the present investigation (fig. 6) indicate clearly that schlieren photographs having a small exposure time (2 microsec.) are inadequate to determine M_{cr} accurately. Figure 6(a) ($M_{30} = 0.513$) shows a disturbance on the 30-percent bump that is similar to the shock formation that occurs at or slightly above M_{cr} (0.524). (Compare with fig. 6(b).) For the condition shown in figure 6(a), the maximum local Mach number, as determined from the pressure-distribution data, is 0.965. A similar phenomenon is observed in the flow past the 10-percent bump, for which $M_{cr} = 0.756$. (Compare figs. 6(f) to 6(h).) In this case the maximum local Mach number is 0.945 for a stream Mach number of 0.733. High-speed moving pictures were not taken for the bumps; however, the disturbances observed in the flow at subcritical Mach numbers are believed to be not stationary. These results are in agreement with results in reference 10 and other results obtained in the Langley 24-inch and rectangular high-speed tunnels. Disturbances can probably be observed, therefore, near the model surface when the local Mach number is of the order of 0.95.

In connection with the occurrence of disturbances in the flow, the conditions under which discontinuities appear in the pressure-distribution diagrams should be considered. The shape of the pressure diagram for the 10-percent bump changed with some indication of a discontinuity at a Mach number of 0.789 corresponding to a maximum local Mach number of 1.10 (fig. 5(e)). In figure 5(f) for the 10-percent bump and figure 4(e) for the 30-percent bump, the maximum local Mach number for both figures is 1.15, and therefore the discontinuity is more definite. Pressure-distribution data from airfoil investigations showed that the first indication of a discontinuity occurred when the maximum local Mach number was equal to or slightly greater than 1.1, whereas a definite discontinuity was evident when the maximum local Mach number was somewhat less than 1.2.

A discontinuity in pressure-distribution diagrams could thus be expected when the local Mach number is approximately 1.15. The discussion of disturbances in the flow past models and discontinuities in pressure-distribution diagrams shows these methods of estimating M_{cr} to be inaccurate.

Because of the general agreement between the present investigation on bumps and previous investigations on airfoils, the experimentally verified parts of the theoretical investigation of reference 1 can be considered to be applicable to airfoils.

CONCLUSIONS

Results of an investigation made in the Langley rectangular high-speed tunnel on the flow past two bumps having thickness-chord ratios of 0.10 and 0.30 indicated the following conclusions:

1. The effects of compressibility on the flow past these specially shaped profiles or bumps were in agreement with previous investigations on airfoils.

2. Reasonably good agreement was found between the experimental results and the symmetrical type of theoretical solution of the flow past the bumps except in the flow over the rear half of the models at supercritical Mach numbers.

3. The large disagreement between the symmetrical type of theoretical solution and the experimentally determined flow over the rear of the models at supercritical speeds indicated a possibility that an asymmetrical type of theoretical solution would be necessary to obtain agreement with the real flow, and such a solution could include mathematical discontinuities in the flow.

4. The "limiting" Mach number was found to have no practical significance in relation to the formation of compression shocks but might have some application to the flow over the forward part of a model where expansions occur at low speeds.

Langley Aeronautical Laboratory
National Advisory Committee for Aeronautics
Langley Field, Va., April 1, 1946

REFERENCES

1. Kaplan, Carl: The Flow of a Compressible Fluid past a Curved Surface. NACA Rep. 794, 1944. (Formerly NACA ARR 3K02.)

2. Ackeret, J.: Über Luftkräfte bei sehr grossen Geschwindigkeiten insbesondere bei ebenen Strömungen. Helvetica Physica Acta, vol. 1, fasc. 5, 1928, pp. 301-322.

3. Prandtl, L.: Remarks on paper by A. Busemann entitled "Profilmessungen bei Geschwindigkeiten nahe der Schallgeschwindigkeit (im Hinblik auf Luftschrauben)," Jahrb. 1928 der WGL, R. Oldenburg (Munich and Berlin), pp. 95-99.

4. Glauert, H.: The Effect of Compressibility on the Lift of an Aerofoil. R. & M. No. 1135, British A.R.C., 1927. (Also, Proc. Roy. Soc. (London), ser. A, vol. 118, no. 779, March 1, 1928, pp. 113-119.)

5. von Kármán, Th.: Compressibility Effects in Aerodynamics. Jour. Aero. Sci., vol. 8, no. 9, July 1941, pp. 337-356.

6. Byrne, Robert W.: Experimental Constriction Effects in High-Speed Wind Tunnels. NACA ACR L4L07a, 1944.

7. Allen, H. Julian, and Vincenti, Walter G.: Wall Interference in a Two-Dimensional-Flow Wind Tunnel with Consideration of the Effect of Compressibility. NACA Rep. 782, 1944. (Formerly NACA ARR 4K03.)

8. Taylor, G. I., and Maccoll, J. W.: The Mechanics of Compressible Fluids. Two-Dimensional Flow at Supersonic Speeds. Vol. III of Aerodynamic Theory, div. H, ch. IV, sec. 3, W. F. Durand, ed., Julius Springer (Berlin), 1935, pp. 241-242.

9. Stack, John: Compressible Flows in Aeronautics. Jour. Aero. Sci., vol. 12, no. 2, April 1945, pp. 127-148.

10. Stack, John, Lindsey, W. F., and Littell, Robert E.: The Compressibility Burble and the Effect of Compressibility on Pressures and Forces Acting on an Airfoil. NACA Rep. 646, 1938.

11. Temple, G., and Yarwood, J.: The Approximate Solution of the Hodograph Equations for Compressible Flow. Rep. No. S.M.E. 3201, British R.A.E., June 1942.

12. Lindsey, W. F.: Effect of Compressibility on the Pressures and Forces Acting on a Modified NACA 65,3-019 Airfoil Having a 0.20-Chord Flap. NACA ACR L5G31a, 1946.

13. Stack, John: Compressibility Effects in Aeronautical Engineering. NACA ACR, Aug. 1941.

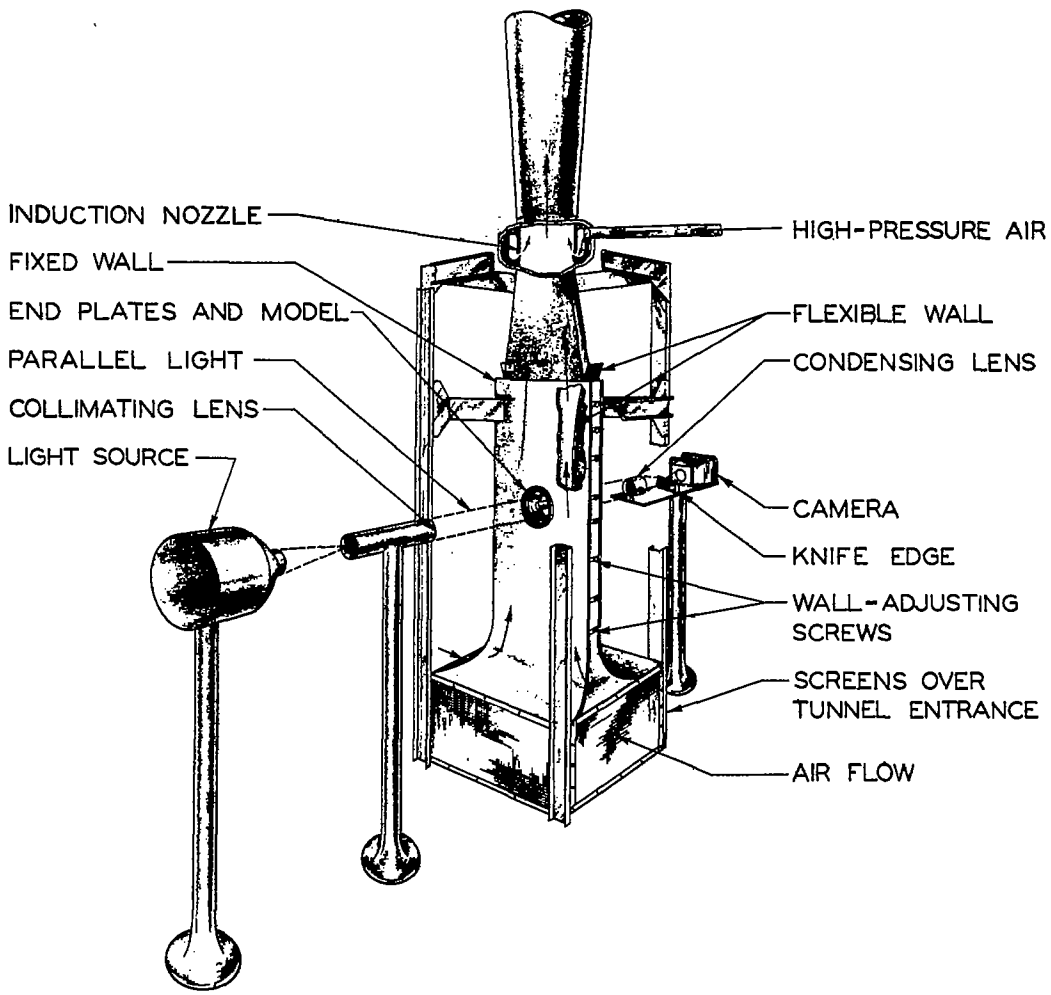

(a) General.

Figure 1.- Schematic diagram of Langley rectangular high-speed tunnel with optical equipment and bump installation.

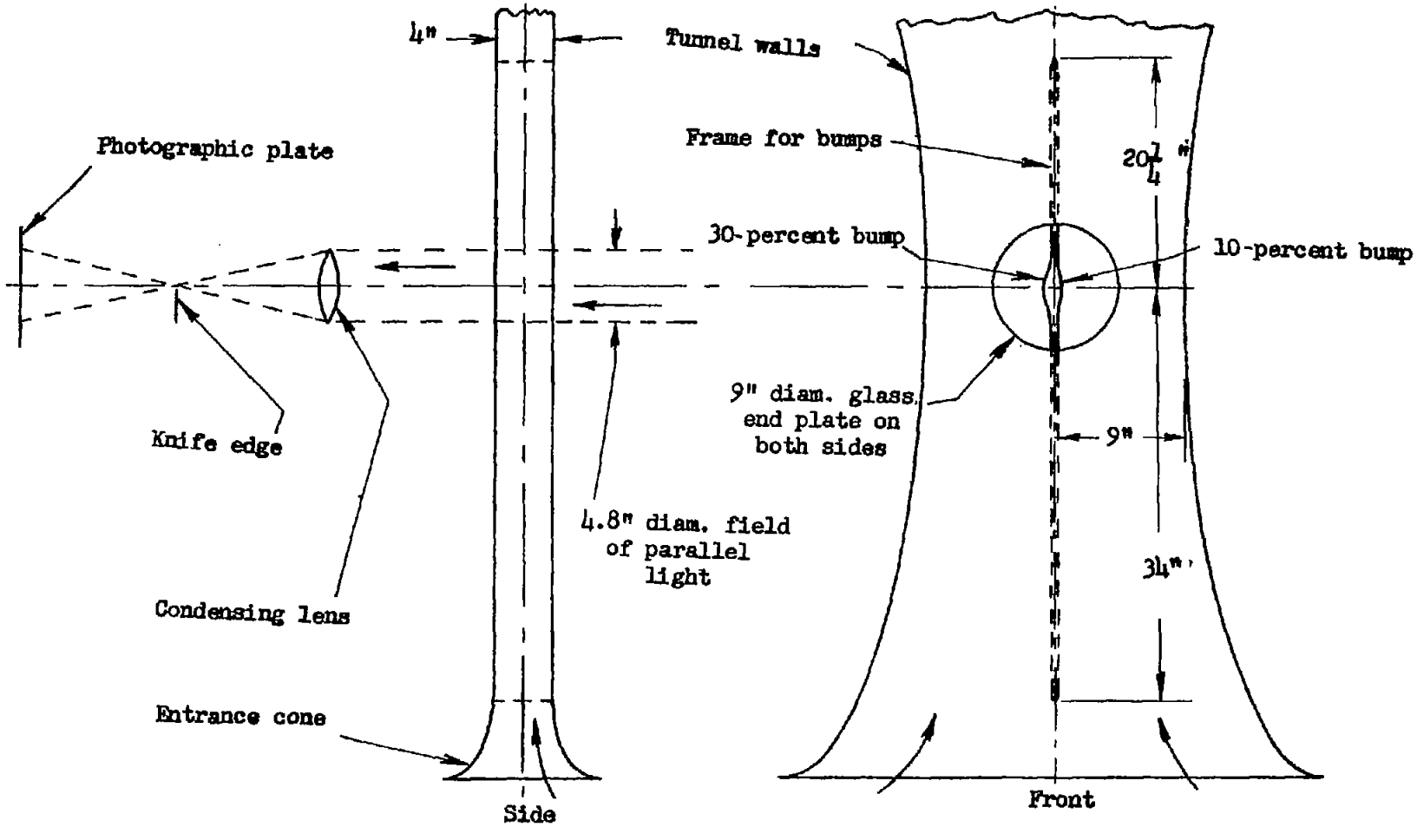

(b) Bump installation.

Figure 1.- Concluded.

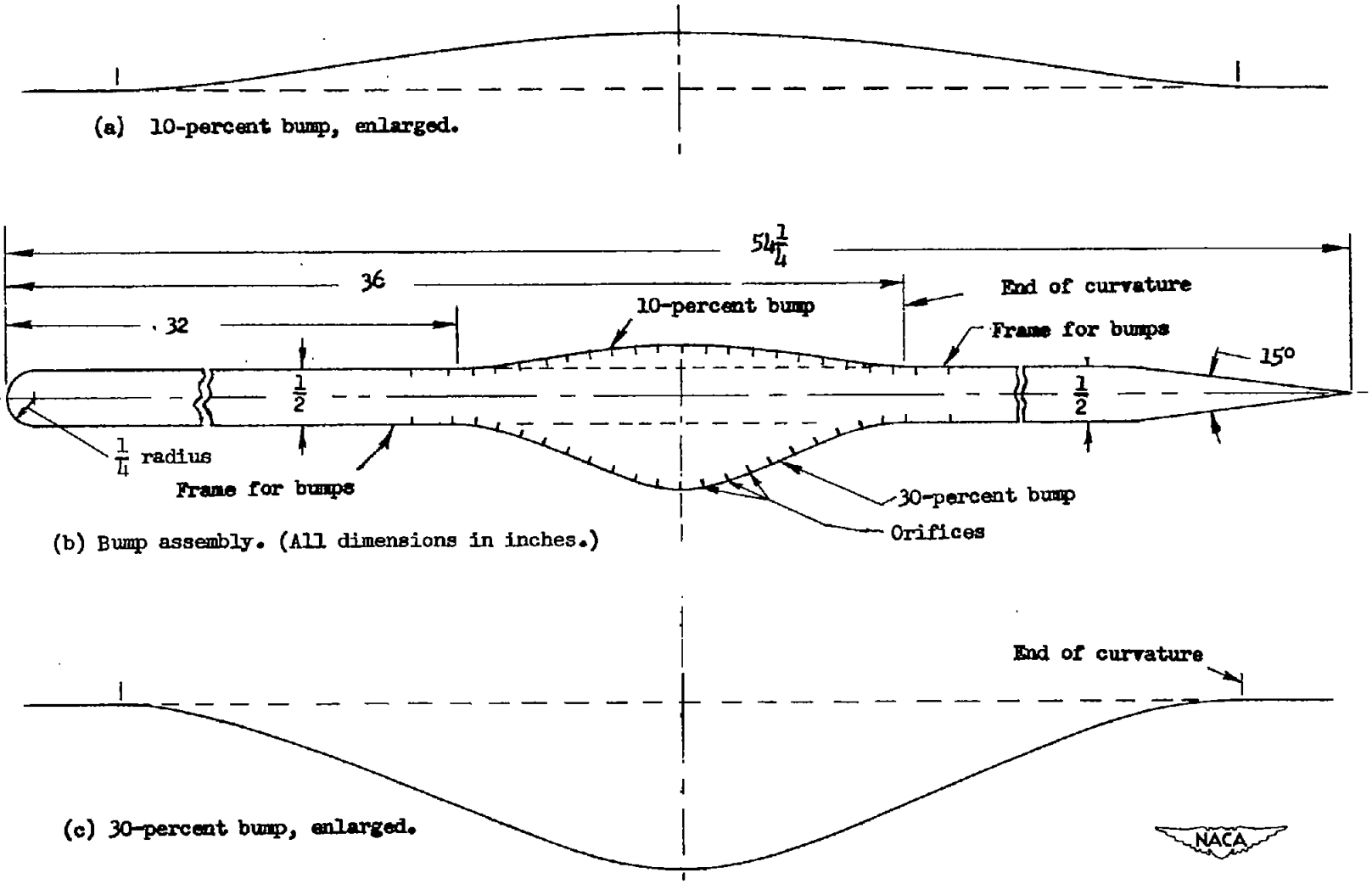

Figure 2.- Bumps and bump assembly.

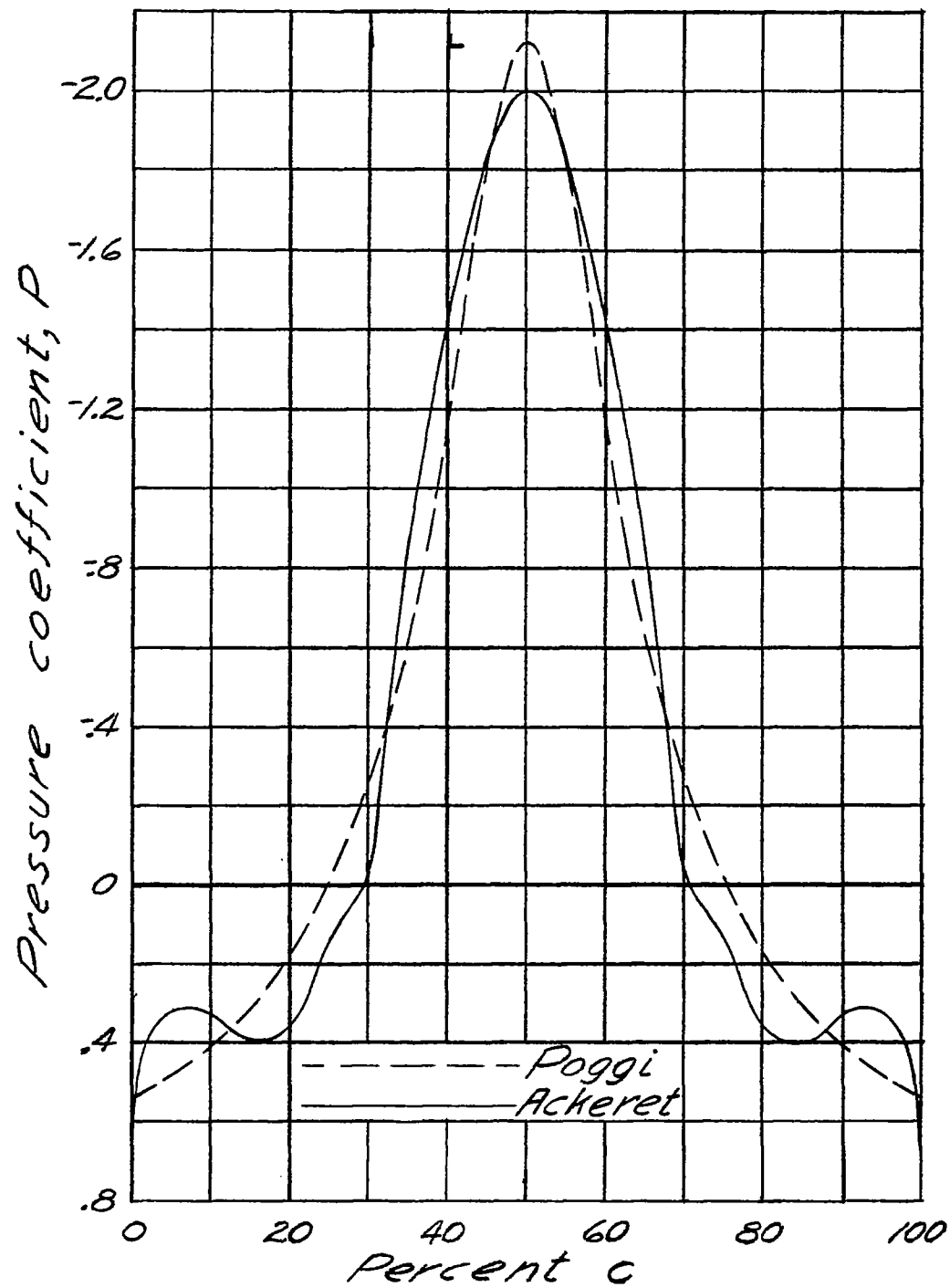

Figure 3.- Comparison of theoretical results from the Poggi and Ackeret methods. 30-percent bump; M = 0.500.

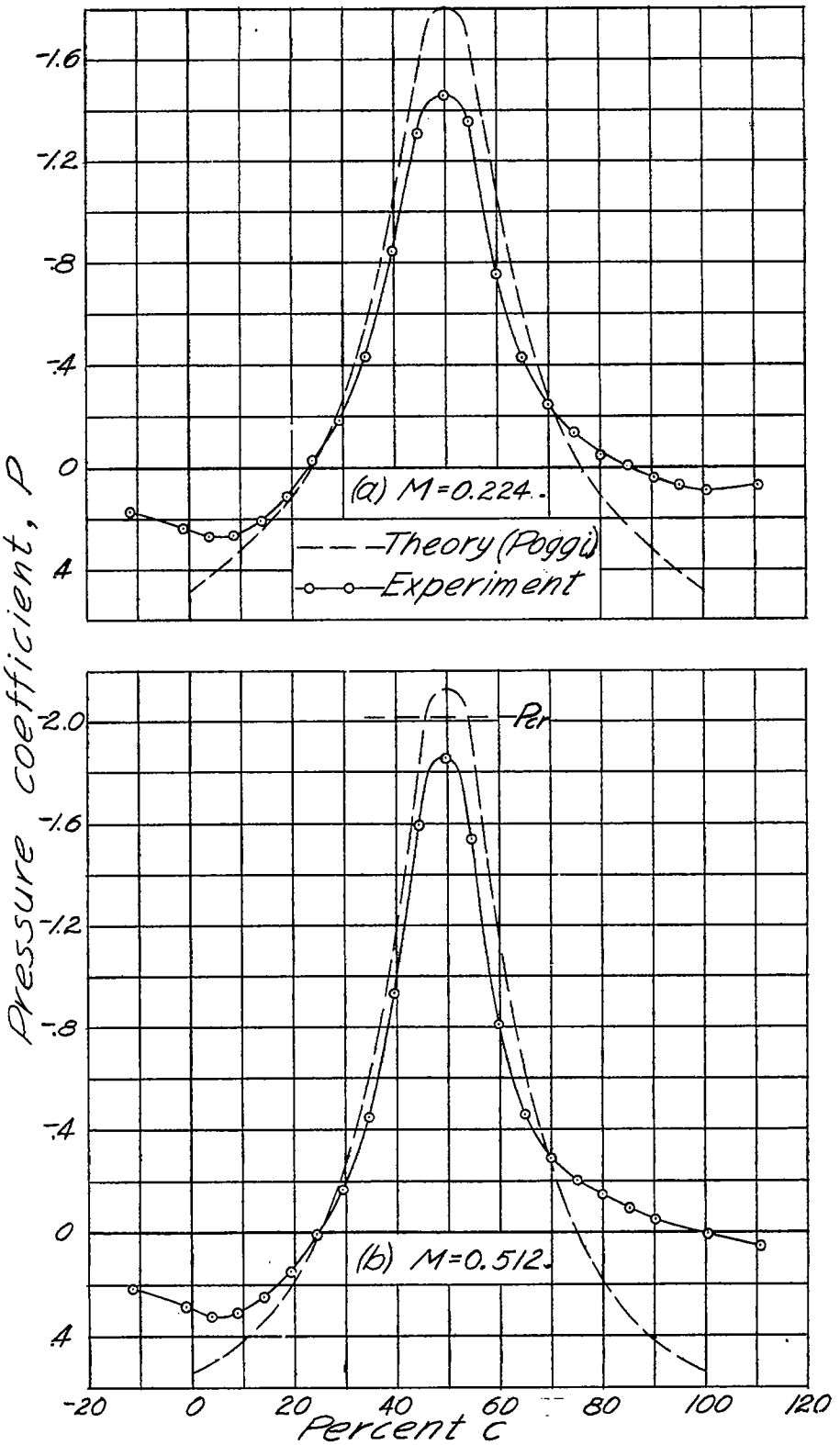

Figure 4.- Pressure distribution over the 30-percent bump.

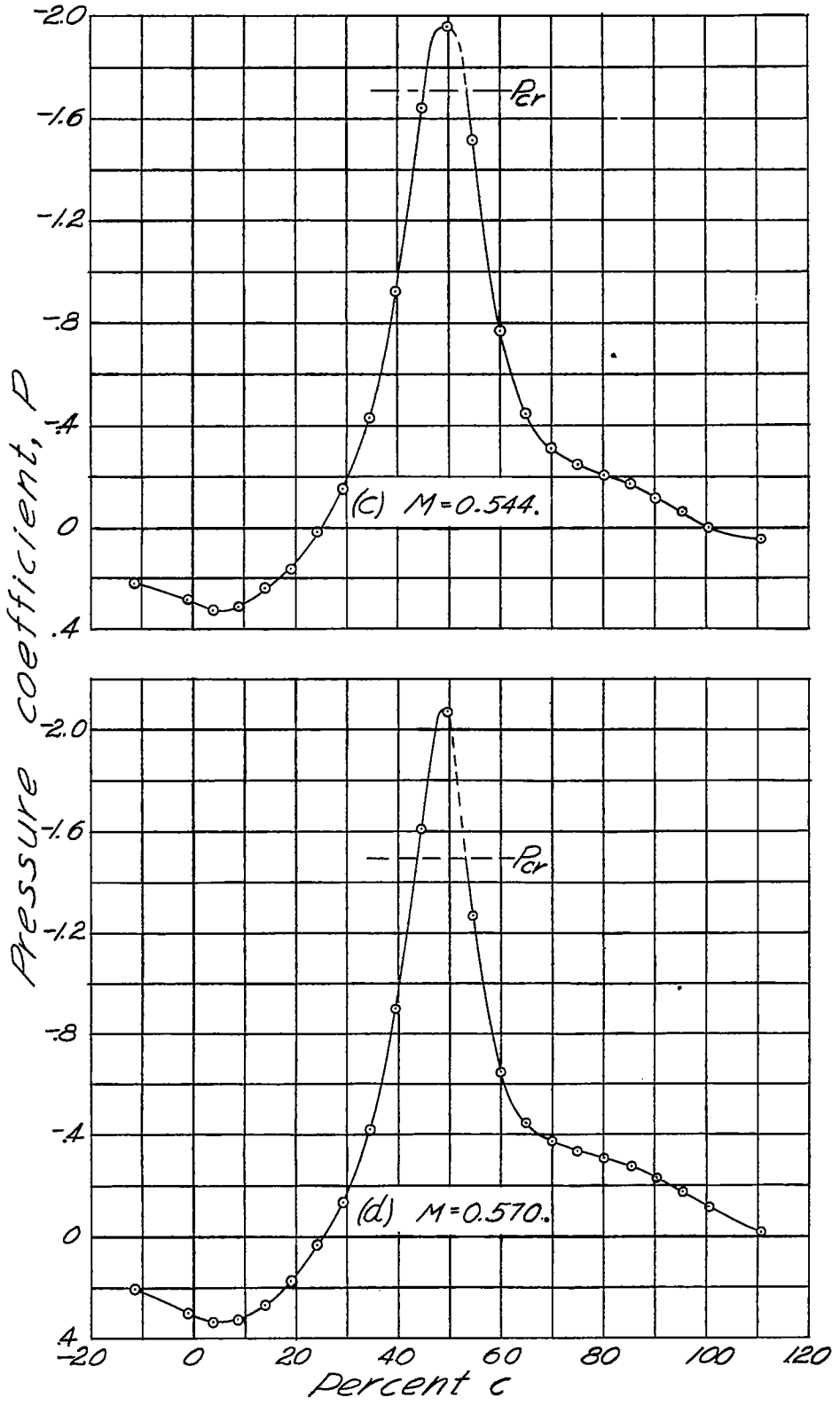

Figure 4.- Continued.

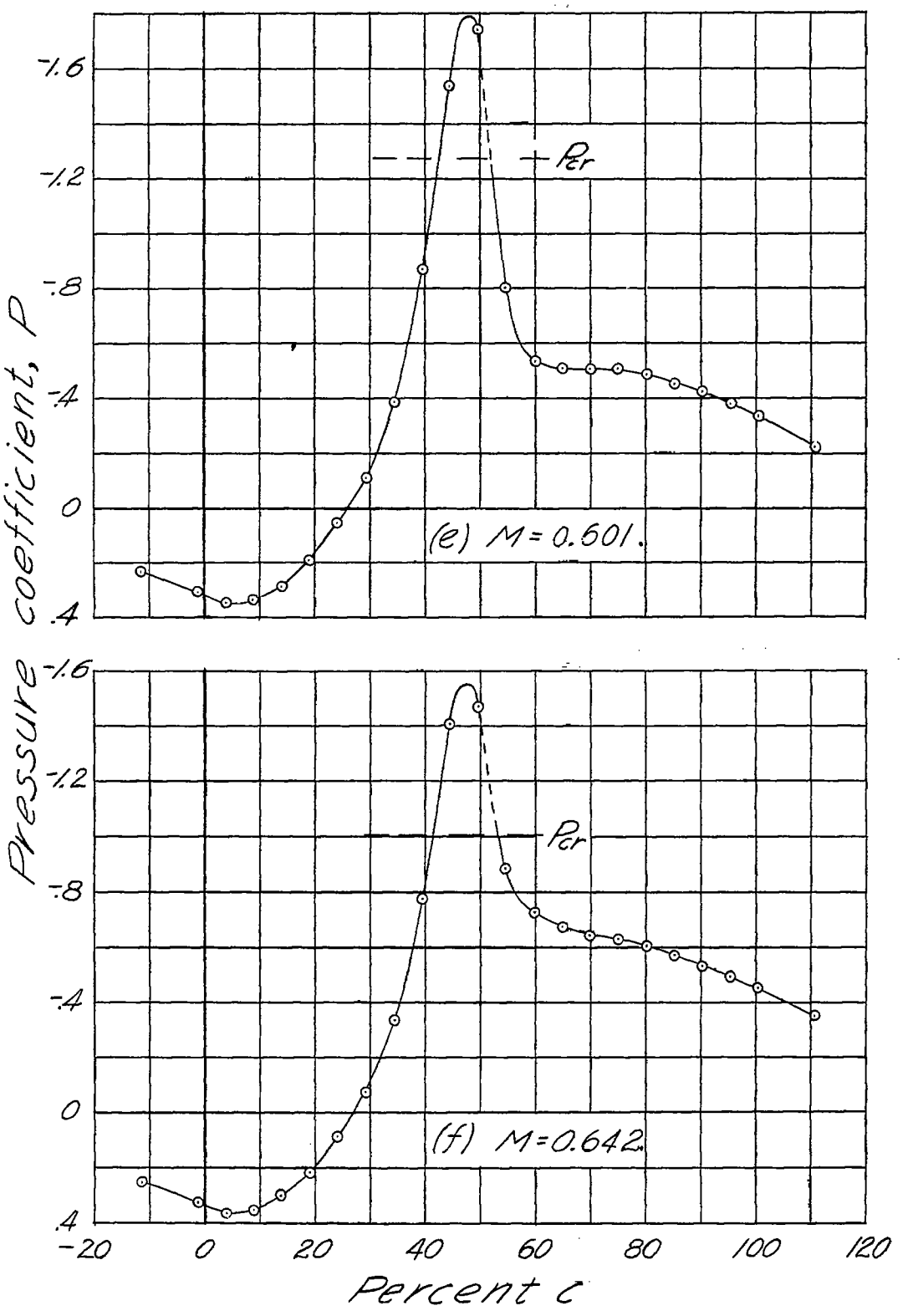

Figure 4.- Continued.

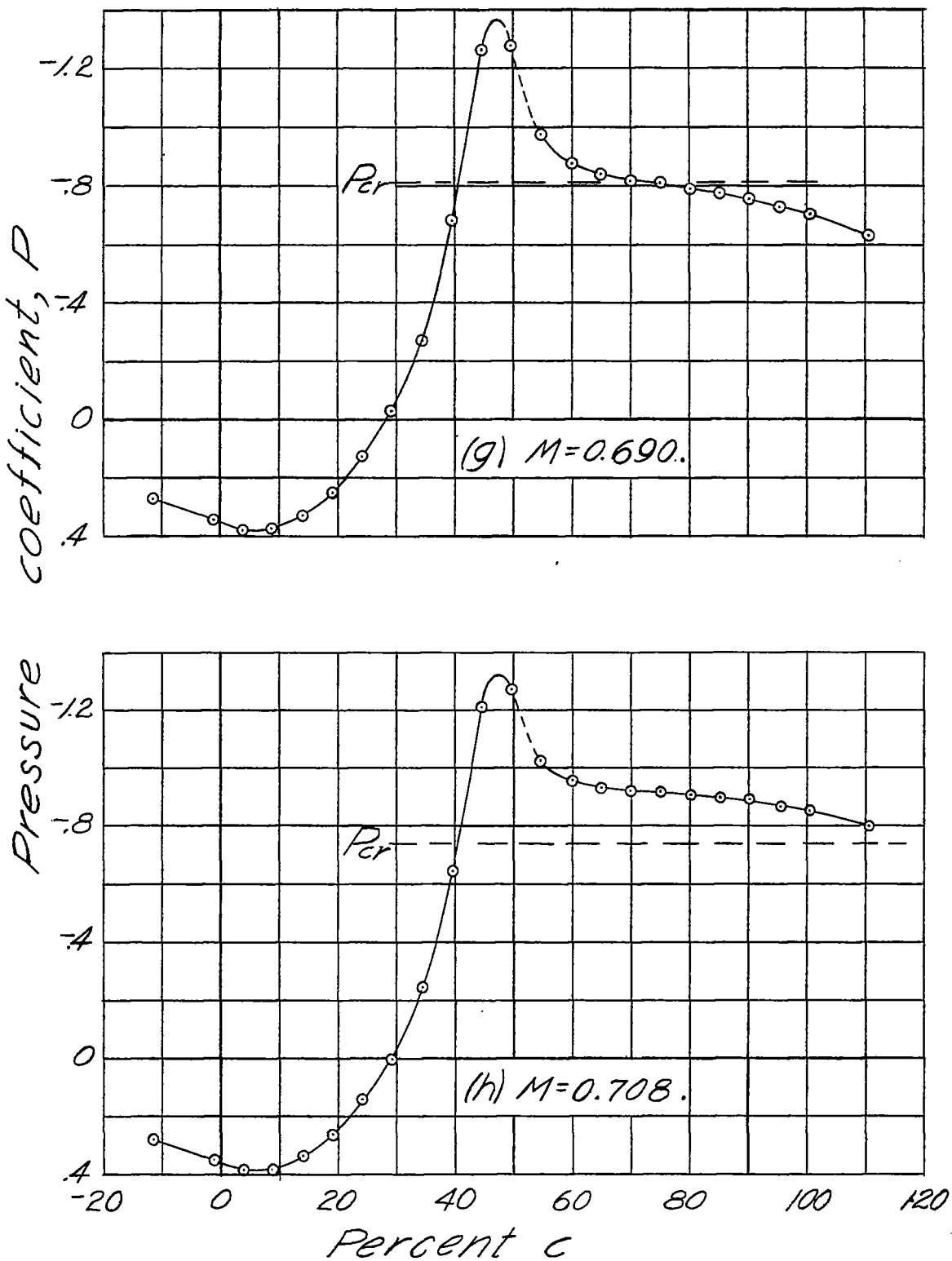

Figure 4.- Concluded.

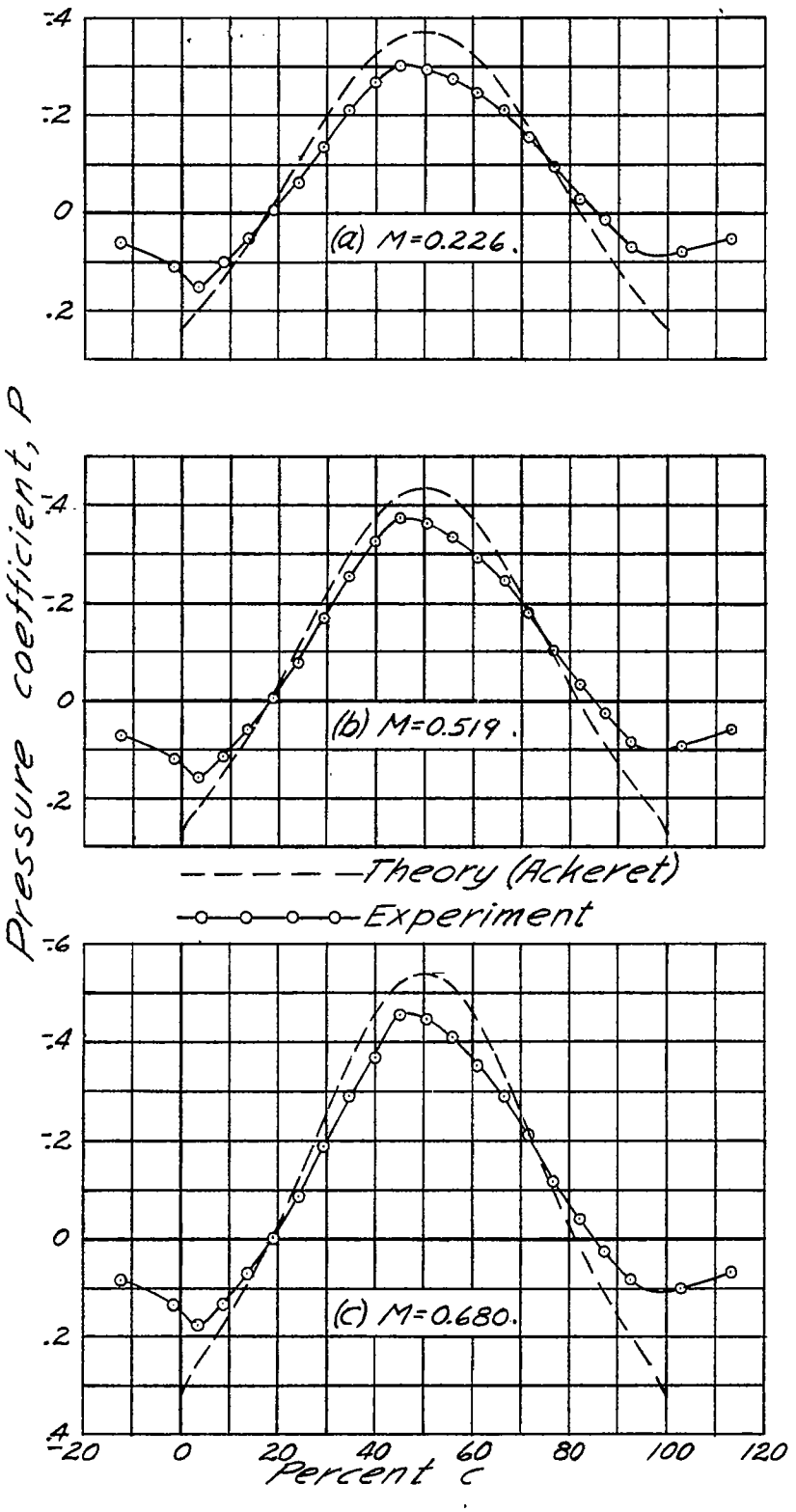

Figure 5.- Pressure distribution over the 10-percent bump.

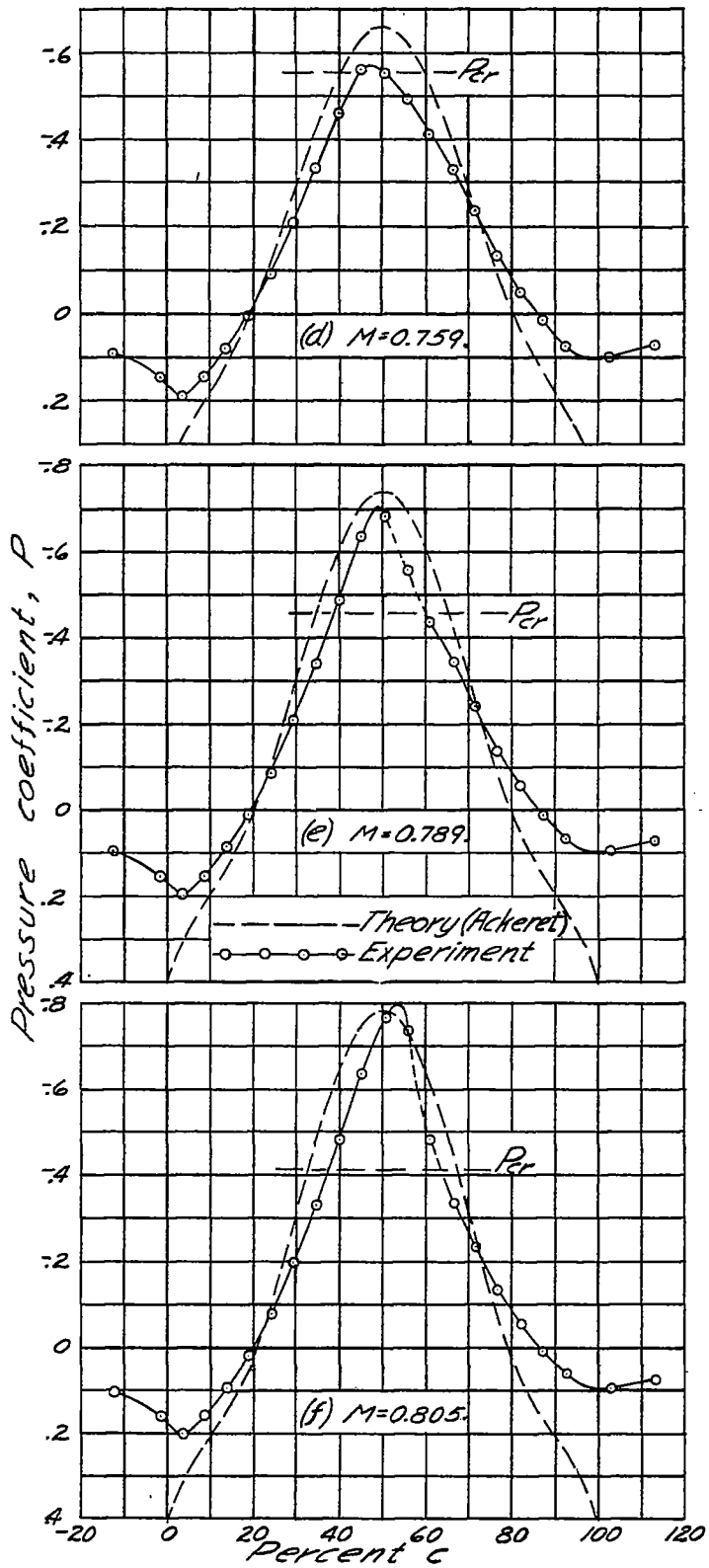

Figure 5.- Continued.

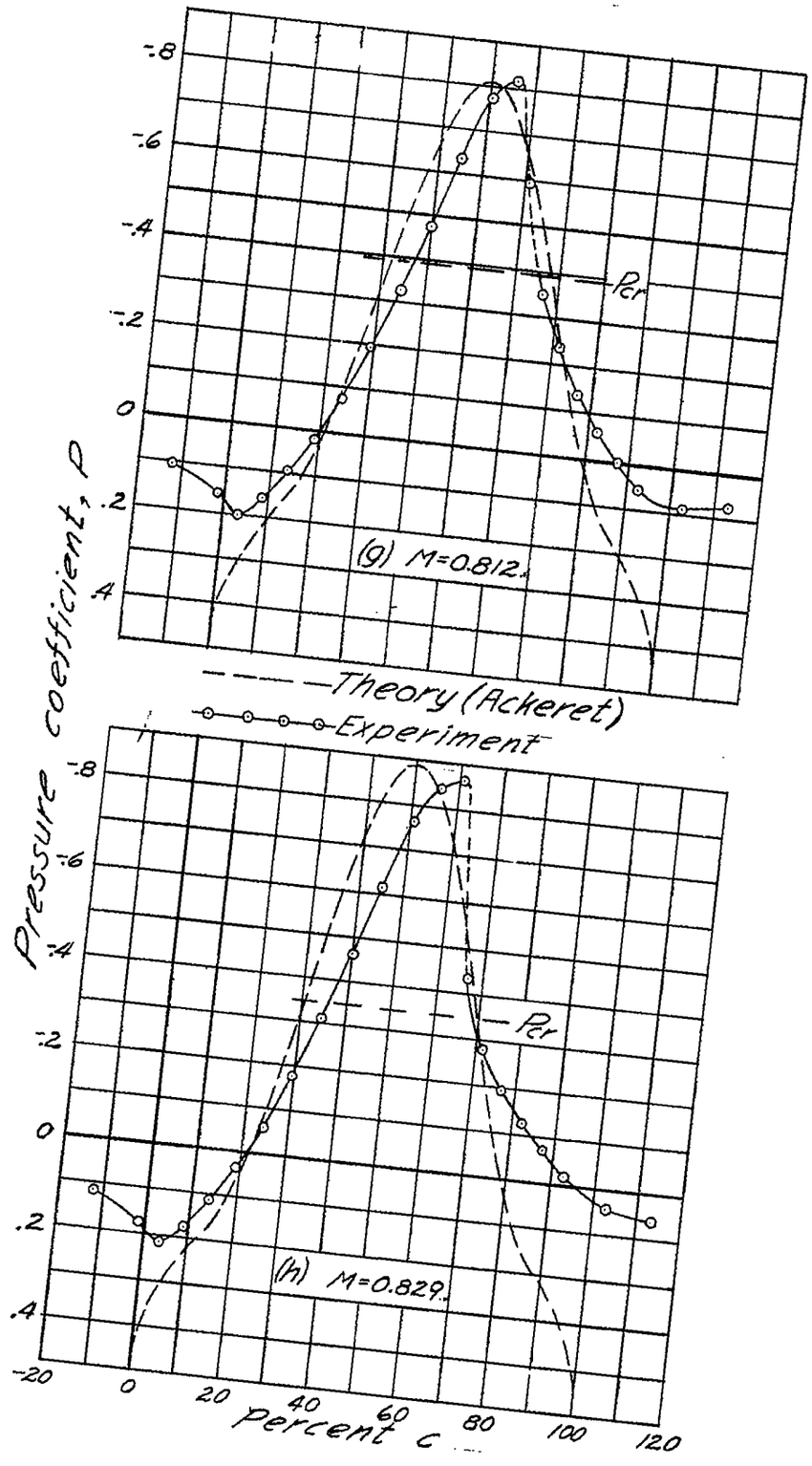

Figure 5.- Concluded.

(a) $M_{10} = 0.520$; $M_{30} = 0.513$.

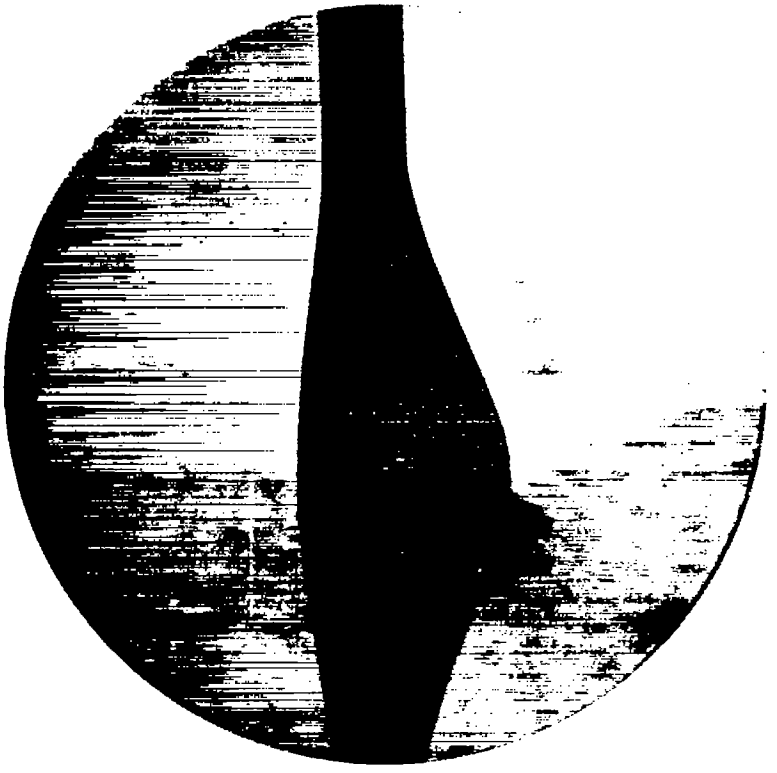

(b) $M_{10} = 0.541$; $M_{30} = 0.534$.

Figure 6.- Schlieren photographs of flow past the 10- and 30-percent bumps.

(c) M_{10} = 0.590; M_{30} = 0.576.

(d) M_{10} = 0.630; M_{30} = 0.606.

Figure 6.- Continued.

(e) $M_{10} = 0.673$; $M_{30} = 0.635$.

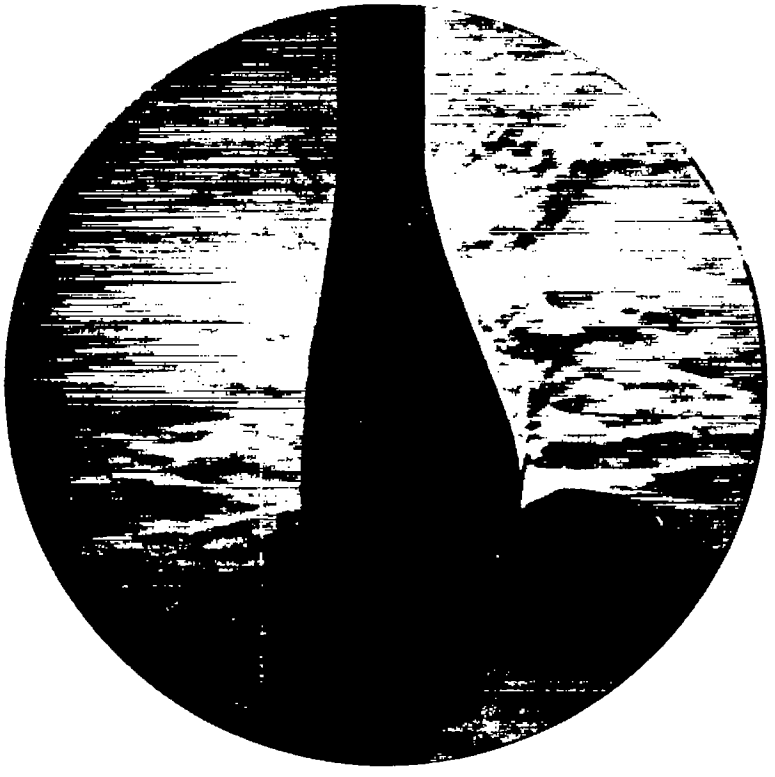

(f) $M_{10} = 0.733$; $M_{30} = 0.670$.

Figure 6.- Continued.

(g) M_{10} = 0.754; M_{30} = 0.680.

(h) M_{10} = 0.785; M_{30} = 0.694.

Figure 6.- Continued.

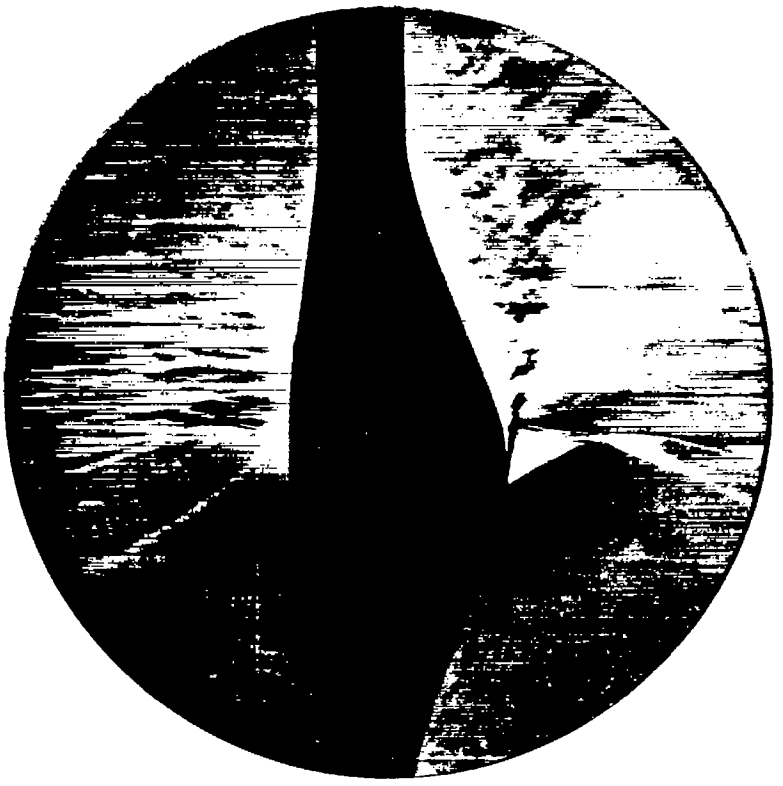

(i) $M_{10} = 0.807$; $M_{30} = 0.701$.

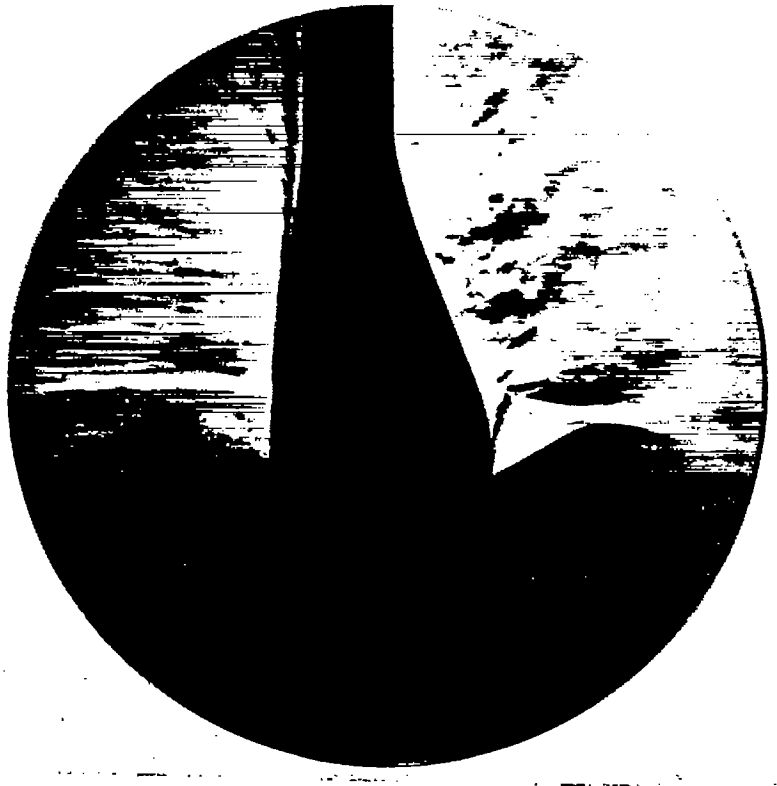

(j) $M_{10} = 0.815$; $M_{30} = 0.705$.

Figure 6.- Continued.

(k) M_{10} = 0.830; M_{30} = 0.710.

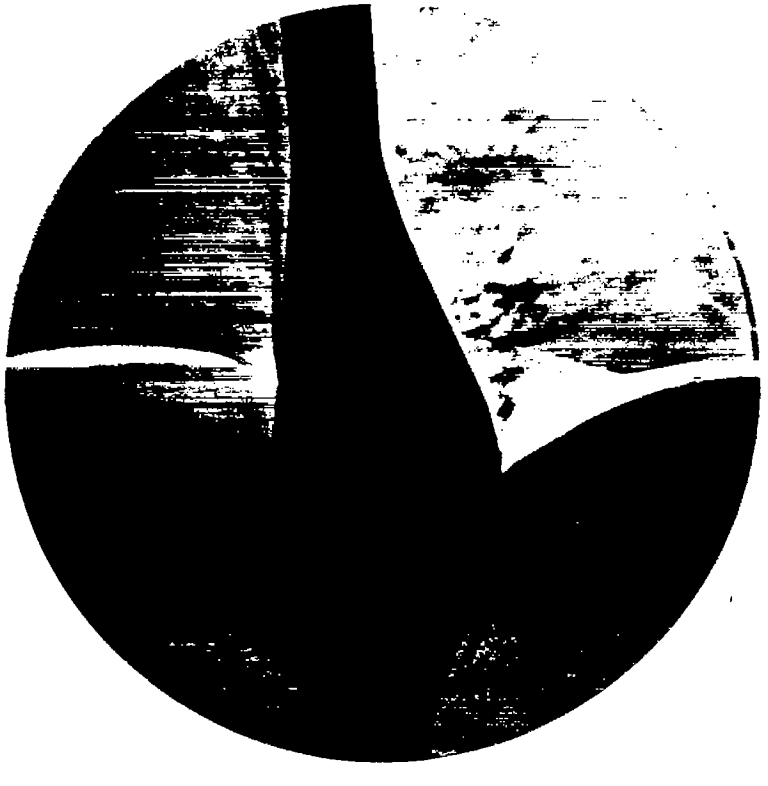

(l) M_{10} = 0.840; M_{30} = 0.714.

Figure 6.- Concluded.

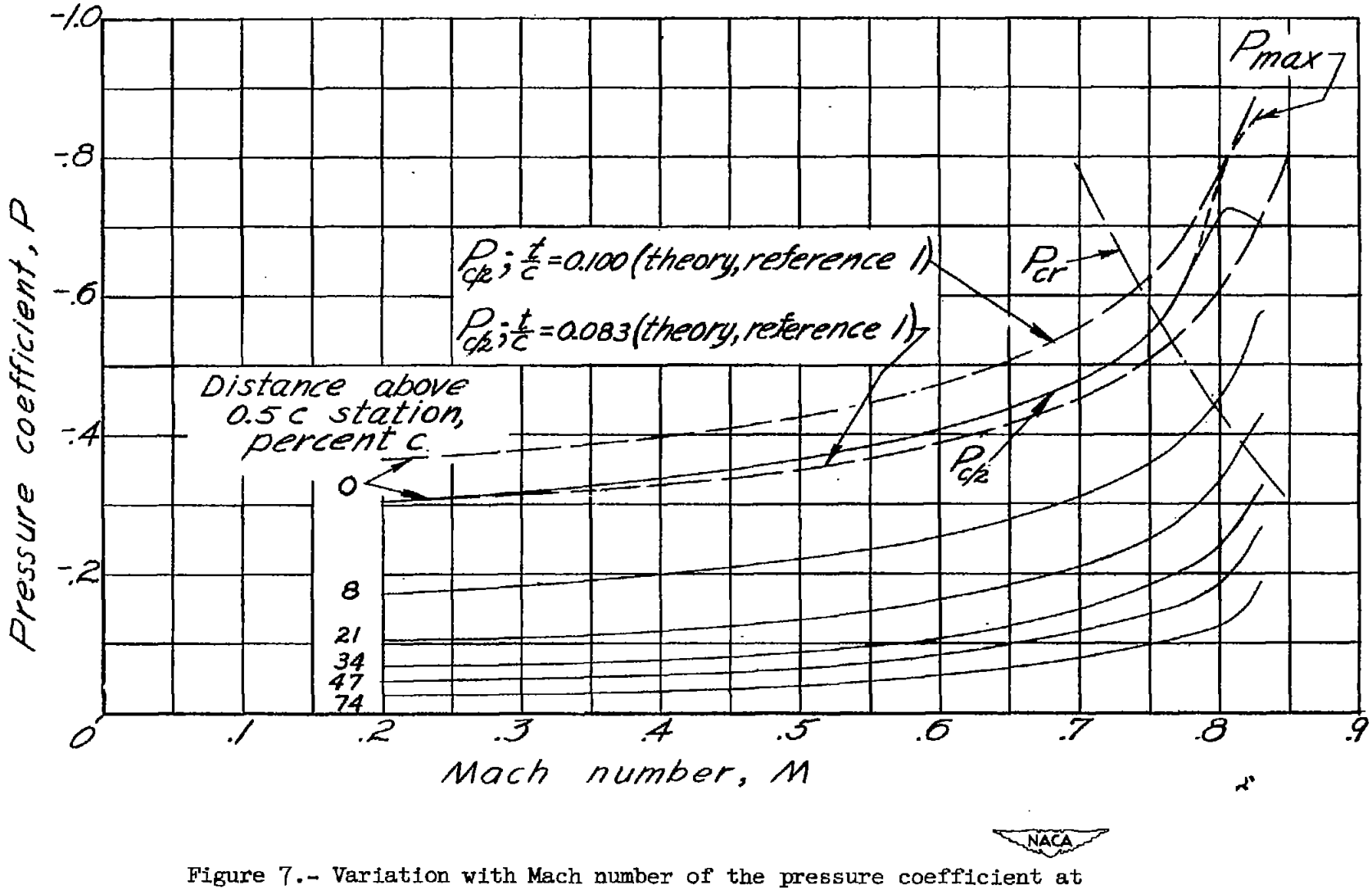

Figure 7.- Variation with Mach number of the pressure coefficient at several locations in the flow field of the 10-percent bump.

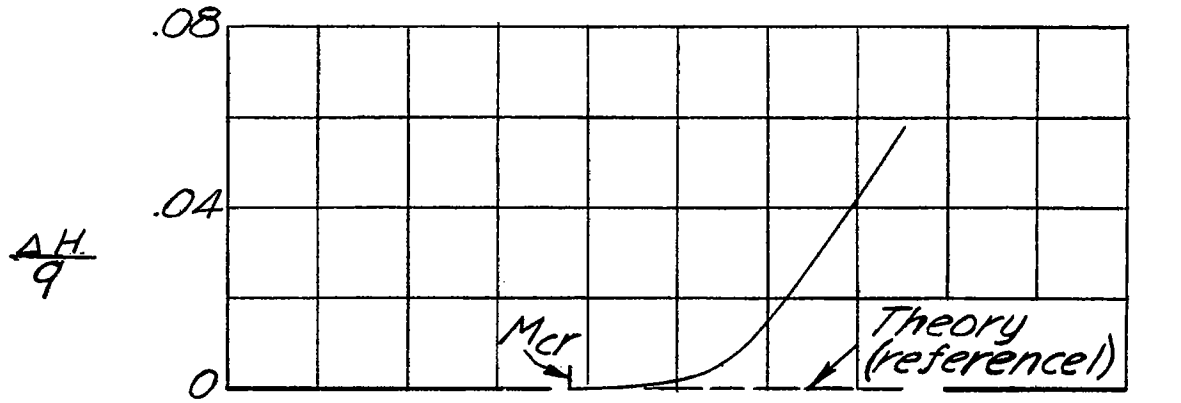

(a) Theoretical loss through normal shock based on measured minimum pressures at model surface.

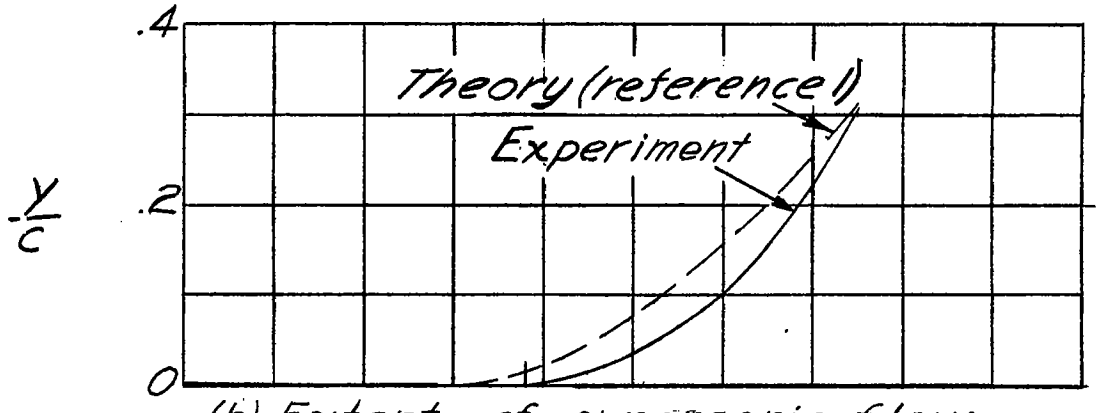

(b) Extent of supersonic flow region above surface of model at 0.5c station.

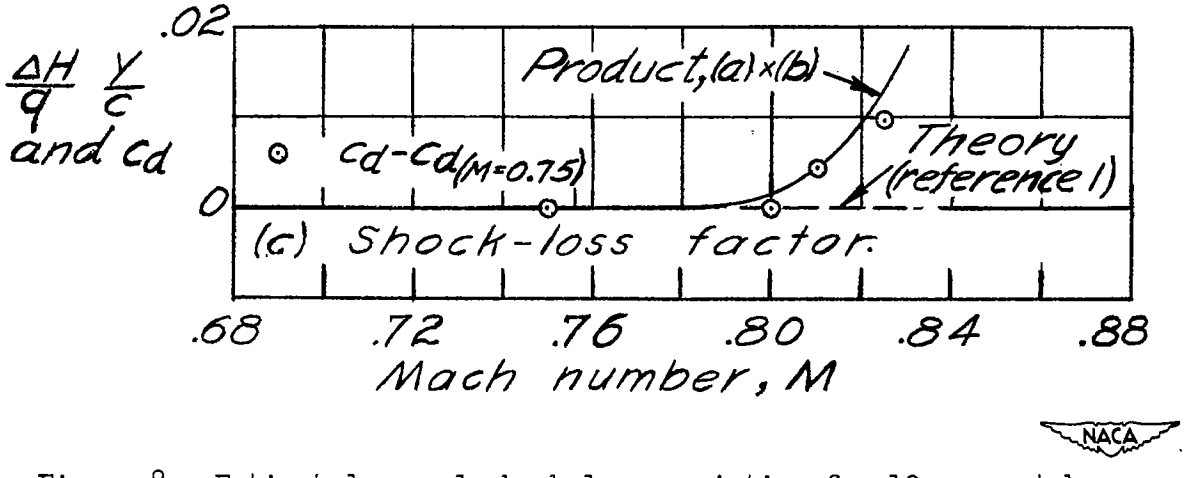

Figure 8.- Estimated normal-shock-loss variation for 10-percent bump.

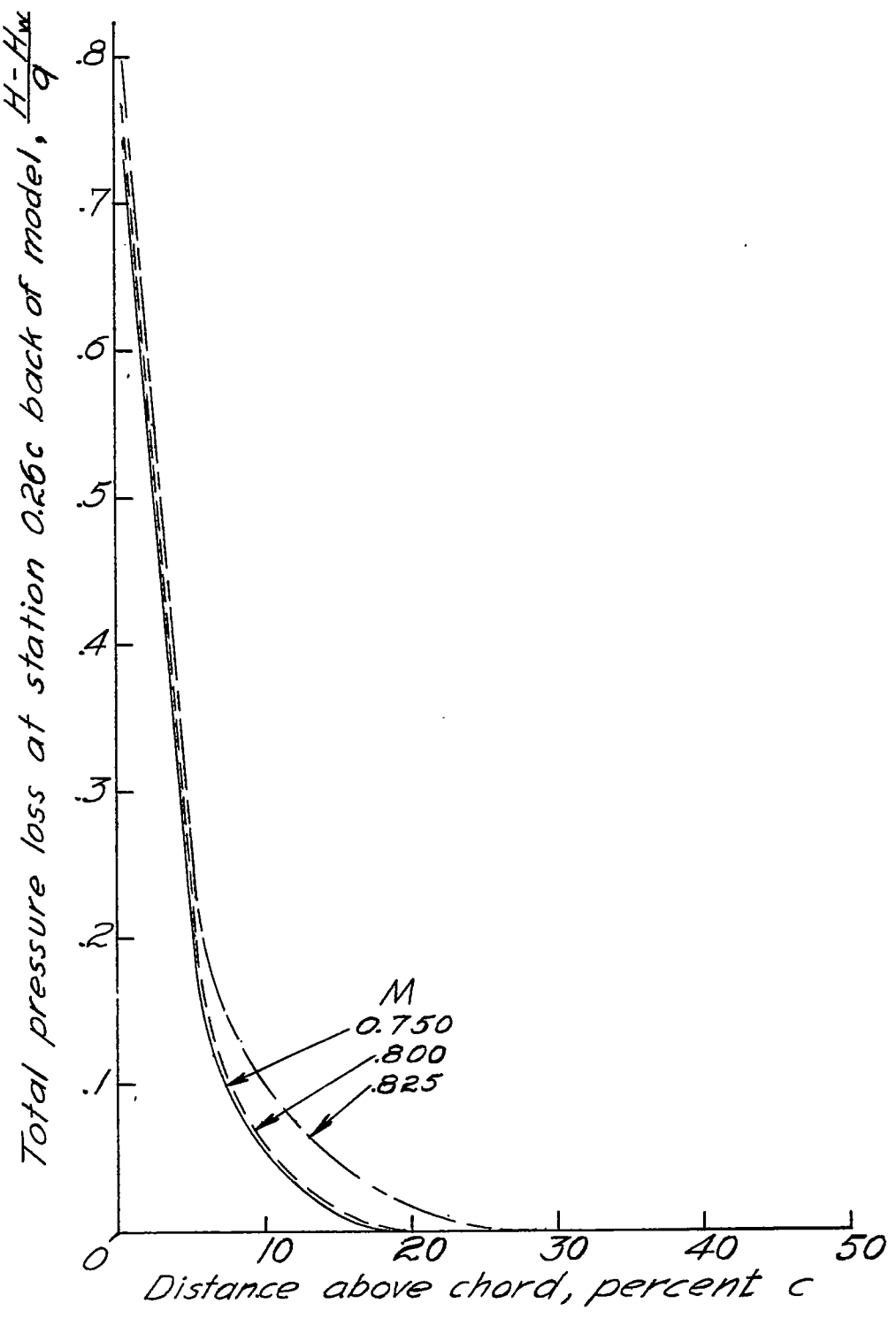

Figure 9.- Total pressure variation across wake of 10-percent bump.

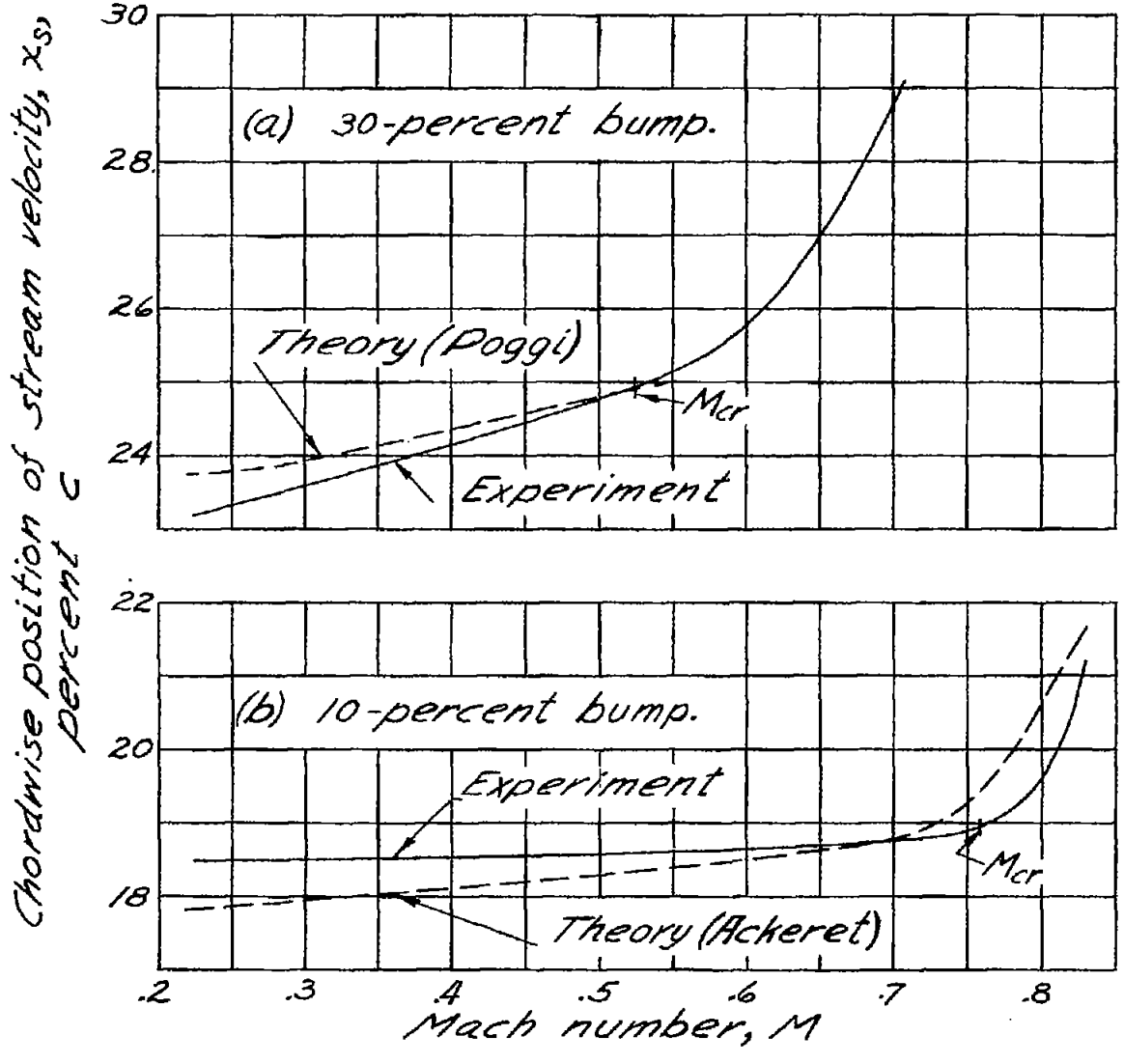

Figure 10.- Position of forward point of stream velocity.